

Article

Simplified Super Twisting Sliding Mode Approaches of the Double-Powered Induction Generator-Based Multi-Rotor Wind Turbine System

Habib Benbouhenni ¹, Nicu Bizon ^{2,3,4,*}, Ilhami Colak ¹, Phatiphat Thounthong ^{5,6}
and Nouredine Takorabet ⁶

- ¹ Department of Electrical & Electronics Engineering, Faculty of Engineering and Architecture, Nisantasi University, Istanbul 34398, Turkey; habib.benbouhenni@nisantasi.edu.tr (H.B.); ilhcol@gmail.com (I.C.)
² Faculty of Electronics, Communication and Computers, University of Pitesti, 110040 Pitesti, Romania
³ Doctoral School, Polytechnic University of Bucharest, 313 Splaiul Independentei, 060042 Bucharest, Romania
⁴ ICSI Energy Department, National Research and Development Institute for Cryogenic and Isotopic Technologies, 240050 Ramnicu Valcea, Romania
⁵ ICSI Renewable Energy Research Centre (RERC), Faculty of Technical Education, King Mongkut's University of Technology North Bangkok, Bangkok 10800, Thailand; phatiphat.t@fte.kmutnb.ac.th
⁶ Group of Research in Electrical Engineering of Nancy (GREEN), University of Lorraine-GREEN, F-54000 Nancy, France; noureddine.takorabet@univ-lorraine.fr
* Correspondence: nicu.bizon@upit.ro

Abstract: This work proposes a new indirect field-oriented control (IFOC) scheme for double-powered induction generators (DPIGs) in multi-rotor wind turbine systems (MRWT_S). The IFOC strategy is characterized by its simplicity, ease of use, and fast dynamic speed. However, there are drawbacks to this method. Among its disadvantages is the presence of ripples in the level of torque, active power, and current. In addition, the total harmonic distortion (THD) value of the electric current is higher compared to the direct torque control method. In order to overcome these shortcomings and in terms of improving the effectiveness and performance of this method, a new algorithm is proposed for the super twisting algorithm (STA). In this work, a new STA method called simplified STA (SSTA) algorithm is proposed and applied to the traditional IFOC strategy in order to reduce the ripples of torque, current, and active power. On the other hand, the inverter of the DPIG is controlled by using a five-level fuzzy simplified space vector modulation (FSSVM) technique to obtain a signal at the inverter output of a fixed frequency. The results obtained from this proposed IFOC-SSTA method with FSSVM strategy are compared with the classical IFOC method which uses the classical controller based on a proportional-integral (PI) controller. The proposed method is achieved using the Matlab/Simulink software, where a generator with a large capacity of 1.5 megawatts is used. The generator is placed in a multi-rotor electric power generation system. On the other hand, the two methods are compared in terms of ripple ratio, dynamic response, durability, and total harmonic distortion (THD) value of the electric current. Through the results obtained from this work, the proposed method based on SSTA provided better results in terms of ripple ratio, response dynamic, and even THD value compared to the classical method, and this shows the robustness of the proposed method in improving the performance and efficiency of the generator in the multi-rotor wind system.

Keywords: double-powered induction generator; indirect field-oriented control; five-level fuzzy simplified space vector modulation; super-twisting algorithm; simplified STA; multi-rotor wind turbine systems



Citation: Benbouhenni, H.; Bizon, N.; Colak, I.; Thounthong, P.; Takorabet, N. Simplified Super Twisting Sliding Mode Approaches of the Double-Powered Induction Generator-Based Multi-Rotor Wind Turbine System. *Sustainability* **2022**, *14*, 5014. <https://doi.org/10.3390/su14095014>

Academic Editor: Miguel Carrión

Received: 28 March 2022

Accepted: 18 April 2022

Published: 22 April 2022

Publisher's Note: MDPI stays neutral with regard to jurisdictional claims in published maps and institutional affiliations.



Copyright: © 2022 by the authors. Licensee MDPI, Basel, Switzerland. This article is an open access article distributed under the terms and conditions of the Creative Commons Attribution (CC BY) license (<https://creativecommons.org/licenses/by/4.0/>).

1. Introduction

Traditionally, field-oriented control (FOC) is among the most widely used control methods in the field of controlling electrical machines, whether they are motors or electric generators, due to its simplicity and ease of implementation. This method is based on the

use of a classic proportional-integral (PI) controller, which gives this method a fast dynamic response. On the other hand, this method is based on the use of the traditional pulse width modulation (PWM) to control the inverter of the machine. There are two types of this method, the direct FOC method and the indirect FOC method [1]. In the field of control, this method was used to control several electrical machines such as the asynchronous motor [2,3] and the synchronous motor [4]. However, this method has been used in the field of renewable energies, as according to the reference [5], this method is among the most widely used methods in the field of generating electric power from wind.

In the FOC method, internal loops are used to control electrical machines, creating ripples in both the current and the torque level of the machine. Moreover, this method gives a slow dynamic response compared to both direct torque control (DTC) and direct power control (DPC) [6]. Among the disadvantages of this method is that the total harmonic distortion (THD) value of the current is much higher compared to both DTC and DPC [7].

In the field of scientific research, there are several solutions that have been suggested in order to improve the performance and effectiveness of the FOC method. Artificial intelligence methods and nonlinear methods are among the most widely used methods. The authors of [8] implemented a super twisting algorithm (STA) on a multi-phase induction motor system using the FOC method where the intention was to minimize the current and torque ripples. Despite the advantages that are achieved using the STA algorithm, compared to the FOC strategy with PI controllers, the main drawback of this proposed method is the unstable frequency and presence of torque and current ripples due to the use of the pulse width modulation (PWM) technique. Another nonlinear FOC strategy is proposed in [9] to control the active and reactive power of the induction generator (IG). According to the study that was completed in [10] with the use of the nonlinear method based on second-order sliding mode control (SOSMC), the results were compared with the classical FOC method based on PI controller, and significant improvements were noticed in both the current and the active power compared to the classical FOC method. The problem with the proposed method is that there is a problem of chattering. However, one of the major drawbacks of employing the SOSMC technique to control electrical machines is that the mathematical form of the studied system must be precisely known. Another nonlinear method was applied to an asynchronous generator controlled by the FOC method. In this proposed method, the third-order sliding mode control (TOSMC) technique is used to compensate for the PI and improve the quality of the active power. One of the results obtained from this work is that the control by TOSMC reduces the chatter problem present in the SMC in addition to reducing the ripples at the level of torque, current, and effective power of the asynchronous generator. In [11], two different methods were combined in principle, where the first method is represented by neural networks, which is characterized by precision and speed of response, while the second method is the TOSMC technique, which is characterized by durability and unaffected by external factors such as noise or change in the parameters of the studied system. The result of combining these two methods is to obtain a more durable method and get excellent quality of the electric current of the induction generator.

In the field of electric machine control, response speed or dynamic response is very important. This response is considered a criterion among the criteria that is selected and differentiated between the control methods. In [12], a new method is proposed under the name of terminal synergetic control in order to improve the performance and effectiveness of the direct FOC strategy for an asynchronous generator integrated into a wind turbine. This proposed method is a new method based on the use of nonlinear error instead of using linear error. The obtained results showed the effectiveness of the proposed method in improving the dynamic response of the induction generator while reducing the ripples of torque and the active power of the induction generator. In [13], a method of artificial intelligence based on the neural networks and fuzzy logic was used to improve the performance and effectiveness of the IFOC strategy of the asynchronous generator, where the classic PI controller was replaced by an intelligent controller under the name of the

neuro-fuzzy controller. The proposed IFOC strategy with the neuro-fuzzy controller is more robust compared to the traditional IFOC strategy. The results showed the effectiveness of the proposed method in improving the THD of stator current value compared to the classical method. Moreover, there is a fast dynamic response to the proposed method, where we find that the response time is much reduced compared to the PI controller. In [14], the author proposed a new FOC strategy based on an adaptive observer to control the induction generator-based wind turbine. The proposed FOC strategy with adaptive observer was experimentally tested on an 11 kW induction generator using a 27 kW DC motor to rotate the generator. The experimental results showed the effectiveness of the proposed FOC method in obtaining a fast dynamic response compared to the classical FOC method.

In this work, a new FOC strategy method is introduced using a new nonlinear method in order to obtain a more robust method and reduce the ripples of torque, active power, and electric current generated by the double-powered induction generator (DPIG). In addition, a new method for the STA algorithm is proposed, where this method is simplified more than the traditional STA method. Thus, a simpler method that can be easily developed and applied to any system regardless of its complexity is designed. The proposed nonlinear method is called the simplified STA (SSTA) algorithm. Among the advantages of this nonlinear method is the fact that the design of the method is not related to the studied system, regardless of what this system will be. This proposed nonlinear method is used in order to improve the performance and effectiveness of the STA method and on the other hand to improve the dynamic response speed of the generator placed in the multi-rotor wind electric power generation system.

The novelty and main contributions of this work accomplished in this paper are summarized in the following points:

- A new super twisting algorithm is proposed and confirmed.
- A new space vector modulation (SVM) scheme is proposed based on the fuzzy logic controller to control the five-level inverter of the DPIG.
- A new IFOC strategy scheme is proposed to control the DPIG-based multi-rotor wind turbine system.
- A new SSTA algorithm is designed to improve the dynamic characteristics of DPIG-based multi-rotor wind turbine systems.

This work is structured as follows. Section 2 presents the dynamic modeling of the multi-rotor wind turbine system. In Sections 3 and 4, the proposed new super twisting algorithm (STA) and the proposed multilevel fuzzy SVM technique are presented. Section 5 presents the traditional IFOC strategy with the PI controller. Section 6 presents the proposed IFOC strategy using the proposed simplified STA controller and five-level fuzzy SVM technique. Finally, Section 7 concludes the work by presenting the main findings and future directions of research, as well as some comments and recommendations.

2. Multi-Rotor Wind Turbine System

The multi-rotor wind turbine is a new technology that has appeared in recent years in order to overcome the problems and defects of the old technology (single-rotor wind turbine). In this new technology, the output torque or power gained from the wind is greater than that gained in the case of a single-rotor wind turbine. In addition, this new technology surpasses the winds generated by wind farms, and thus the yield is greater compared to the single-rotor wind turbine [15]. Figure 1 represents the electric power generation system using the DPIG placed in the electric power generation system using a multi-rotor wind turbine.

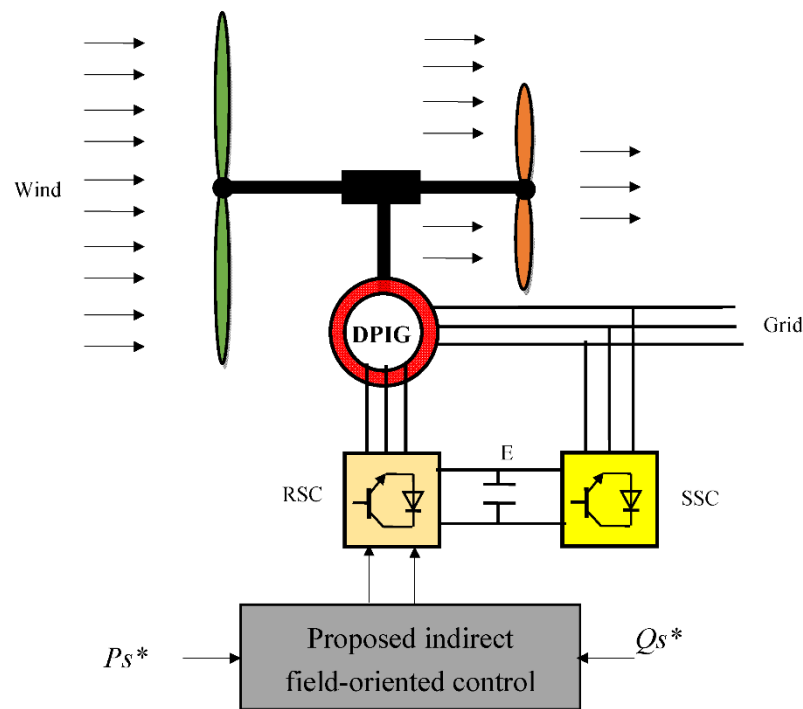


Figure 1. Structure of the multi-rotor wind turbine system.

In the studied wind system, a large-power DFIG (1.5 megawatts) is used. This generator is fed from the electrical network using two different inverters. The first inverter is on the side of the electrical network to convert alternating voltage into constant voltage, while the second inverter, which is on the side of the DFIG, aims to convert the constant voltage resulting from the first inverter into alternating voltage. To rotate the generator, a dual-rotor wind turbine is used.

The two-rotor wind turbine is used in this work in order to increase the energy gained from the wind. On the other hand, a dual-rotor wind turbine is two turbines linked together forming one turbine. The two turbines have the same axis of rotation, and the torque and energy resulting from them can be expressed by the following equations:

$$P_t = P_{ST} + P_{LT} \quad (1)$$

$$T_t = T_{ST} + T_{LT} \quad (2)$$

where T_t is the output torque of the dual-rotor wind turbine, T_{LT} and T_{ST} are the output torque of the large and small wind turbines, P_t is the output mechanical power of the dual-rotor wind turbine, P_{LT} and P_{ST} are the output mechanical power of the large and small wind turbine torque.

The term torque for both large and small turbines is shown in Equations (3) and (4), respectively [16].

$$T_{LT} = \frac{C_p}{2\lambda_{LT}^3} \rho \cdot \pi \cdot R_{LT}^5 \cdot w_{LT}^2 \quad (3)$$

$$T_{ST} = \frac{C_p}{2\lambda_{ST}^3} \rho \cdot \pi \cdot R_{ST}^5 \cdot w_{ST}^2 \quad (4)$$

From the two equations, it can be seen that the torque of the two turbines is related to each of the air density (ρ), coefficient of power (C_p), the mechanical speed of the small and large turbines (w_{ST} and w_{LT}), the blade radius of the small and large turbines (R_{ST} , R_{LT}), and the tip speed ratio of the small and large turbines (λ_{ST} and λ_{LT}).

The energy gained from wind by a dual-rotor turbine is related to the power factor, the value of which is related to pitch angle (β) and tip speed ratio (λ). This parameter can be expressed by the following equation:

$$C_p(\beta, \lambda) = \frac{1}{0.08\beta + \lambda} + \frac{0.035}{\beta^3 + 1} \quad (5)$$

The terms of the energy produced by both the small turbine and the large turbine are shown in Equations (6) and (7), respectively [17].

$$P_{ST} = \frac{C_p(\beta, \lambda)}{2} \rho \cdot S_{ST} \cdot w_{ST}^3 \quad (6)$$

$$P_{LT} = \frac{C_p(\beta, \lambda)}{2} \rho \cdot S_{LT} \cdot w_{LT}^3 \quad (7)$$

The value of the tip speed ratios of the small turbine and the large turbine are given in Equations (8) and (9), respectively [15].

$$\lambda_{ST} = \frac{w_{ST} \cdot R_{ST}}{V_{ST}} \quad (8)$$

$$\lambda_{LT} = \frac{w_{LT} \cdot R_{LT}}{V_{LT}} \quad (9)$$

The values of the tip speed ratios for a large and a small turbine are related to the wind speed (V_{ST} and V_{LT}), The speed of the large and small turbine (w_{ST} and w_{LT}), and the blade radius of the small and large turbines (R_{ST} , R_{LT}).

The wind speed between the large and small turbines is different from the wind speed before the large turbines. The wind speed can be calculated at any point between the turbines given the following relationship [17]:

$$V_x = V_{LT} \left(1 - \frac{1 - \sqrt{(1 - C_T)}}{2} \left(1 + \frac{2x}{\sqrt{1 + 4x^2}} \right) \right) \quad (10)$$

The wind speed of the small turbine is related to the wind speed of the large turbine (V_{LT}) and a constant value ($C_T = 0.9$), as well as the separation distance (x) between the large and small turbine. In this case, this distance between the center of the large and small turbine is 15 m [15].

In this work, a multi-rotor turbine is used to drive an DFIG. The latter was used in this work, and this is due to the advantages that distinguish it compared to other generators. As it is known, the DFIG is characterized by durability, easy control, and low cost.

In order to give the generator a mathematical form, the park transformation is used. To give the generator the mathematical form, the equations of voltage, flux, and mechanical equation are used. In addition, the torque equation is given for the generator, since torque is related to both current and flux. Quadrature and direct rotor voltages are shown in Equation (11). The direct and quadrature rotor flux are related to the stator/rotor current and are represented in Equation (12) [18–20].

$$\begin{cases} V_{dr} = R_r I_{dr} - \omega_r \Psi_{qr} + \frac{d}{dt} \Psi_{dr} \\ V_{qr} = R_r I_{qr} + \omega_r \Psi_{dr} + \frac{d}{dt} \Psi_{qr} \end{cases} \quad (11)$$

$$\begin{cases} \Psi_{dr} = L_r I_{dr} + M I_{ds} \\ \Psi_{qr} = M I_{qs} + L_r I_{qr} \end{cases} \quad (12)$$

Equation (13) represents each of the direct and quadrature stator voltages. Through this equation, the tension is related to stator resistance (R_s), direct and quadrature stator current (I_{ds} and I_{qs}), direct and quadrature stator (Ψ_{qs} and Ψ_{ds}), and electrical pulsation

of the stator (w_s). The direct and quadrature stator flux are represented in Equation (14). These two fluxes are related to both the inductance of the stator (L_s), direct and quadrature rotor current (I_{dr} and I_{qr}), and direct and quadrature rotor current (I_{ds} and I_{qs}).

$$\begin{cases} V_{qs} = R_s I_{qs} + w_s \Psi_{ds} + \frac{d}{dt} \Psi_{qs} \\ V_{ds} = R_s I_{ds} - w_s \Psi_{qs} + \frac{d}{dt} \Psi_{sd} \end{cases} \quad (13)$$

$$\begin{cases} \Psi_{qs} = M I_{qr} + L_s I_{qs} \\ \Psi_{ds} = L_s I_{ds} + M I_{dr} \end{cases} \quad (14)$$

The value of the generated torque (T_e) is related to rotor current, the number of pole pairs (p), and stator flux and its expression can be given by Equation (15) [19].

$$T_e = 1.5 p \frac{M}{L_s} (-\Psi_{sd} I_{rq} + \Psi_{sq} I_{rd}) \quad (15)$$

The active power and the reactive power of the generator are represented in the Equation (16). The active power is related to stator current and stator voltage, and the same is related to the reactive power.

$$\begin{cases} P_s = 1.5 (V_{qs} I_{qs} + I_{ds} V_{ds}) \\ Q_s = 1.5 (-I_{qs} V_{ds} + V_{qs} I_{ds}) \end{cases} \quad (16)$$

The mechanical part of the DPIG is represented by Equation (17). This equation gives the relationship between torque and speed (Ω).

$$T_e = J \frac{d\Omega}{dt} + f\Omega + T_r \quad (17)$$

where T_r is the load torque, Ω is the mechanical rotor speed, J is the inertia, f is the viscous friction coefficient.

3. Simplified STA Controller

Super twisting algorithm (STA) is among the most widely used nonlinear methods in the field of electrical machine control, due to its durability and ease of implementation [21]. The use of the STA algorithm in automated systems gives great effectiveness in improving the performance and efficiency of electrical machines. On the other hand, the STA algorithm is a type of SOSMC technique. The STA algorithm reduces chattering problems compared to the traditional SMC technique [22]. Equation (18) represents the super twisting algorithm [23]. The classical STA algorithm can be illustrated in Figure 2.

$$\begin{cases} u = K_p |e|^r \text{Sign}(e) + u_1 \\ \frac{du_1}{dt} = K_i \text{Sign}(e) \end{cases} \quad (18)$$

where e is the error or surface, r is the exponent defined for the traditional STA regulator, and K_i and K_p are positive values.

In this work, a new look is given to the STA algorithm in order to further simplify the algorithm and increase its dynamic response. Equation (19) represents the proposed method for the traditional STA algorithm which has been called the simplified STA algorithm (SSTA). The Lyapunov theory is used in order to check the stability of this proposed SSTA controller. This proposed SSTA algorithm is simpler compared to the traditional STA technique.

$$w = K \times |e|^r \times \text{Sign}(e) \quad (19)$$

$$e \times \dot{e} < 0 \quad (20)$$

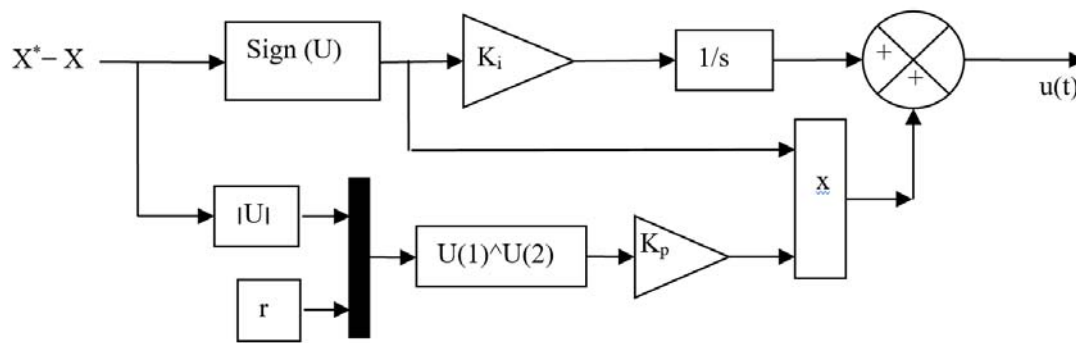


Figure 2. Structure of the traditional STA algorithm.

Figure 3 illustrates the working principle of the proposed SSTA controller. Through this figure, the proposed SSTA controller can be implemented easily and inexpensively and can be applied to any system. Moreover, this controller does not require the mathematical form of the studied system.

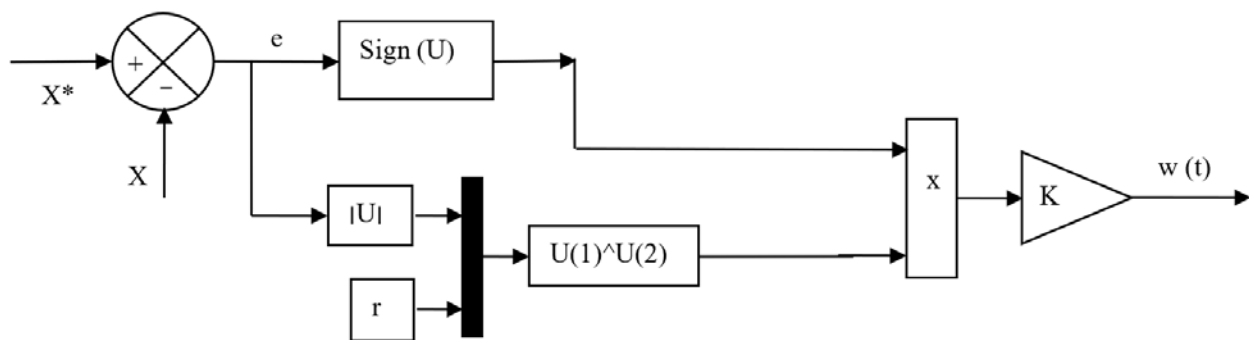


Figure 3. Structure of the proposed SSTA technique.

4. Proposed Five-Level Fuzzy SVM Strategy

Traditionally, the SVM technique is among the most used methods for controlling reflectors and this is because of the results it offers compared to other methods such as the PWM technique [24]. In this method, the calculation of reference voltage and zones is relied upon, which makes this method more complicated, especially in the case of a multi-level inverter [25]. To overcome this problem, a new idea for this method was presented in [26], where the calculation of the maximum and minimum values of the three-phase feeding voltages was used in this proposed method. In this proposed method, the reference tension is not used or calculated as well as the regions where the reference tension is present. This proposed method in [26] is simpler and more intuitive compared to the classical SVM method. In this part, the proposed fuzzy SVM technique is used to control a five-level inverter for an asynchronous generator placed in a multi-turbine wind system. This proposed method of controlling a 5-level inverter is illustrated in Figure 4. The proposed method was used in [27] in order to give the five-level SVM technique.

In this proposed fuzzy SVM technique, twelve hysteresis comparators and four trigonometric signals are used. The use of hysteresis comparators in this proposed SVM method creates a signal at the inverter output of a non-fixed frequency. In order to overcome this drawback, fuzzy logic algorithm (FLA) is used instead of using hysteresis comparators. The use of the FLA leads to a signal at the output of the inverter with a fixed frequency, thus reducing the ripples of both the current and the active power. The SVM method based on the FLA technique proposed in this work is illustrated in Figure 5. With this figure, the proposed method of SVM for controlling the five-level inverter is simpler compared to using the classical five-level SVM method using the calculation of reference voltage and zones. In this method, twelve FLA techniques are used in order to obtain control signals for the inverter transistors (IGBTs).

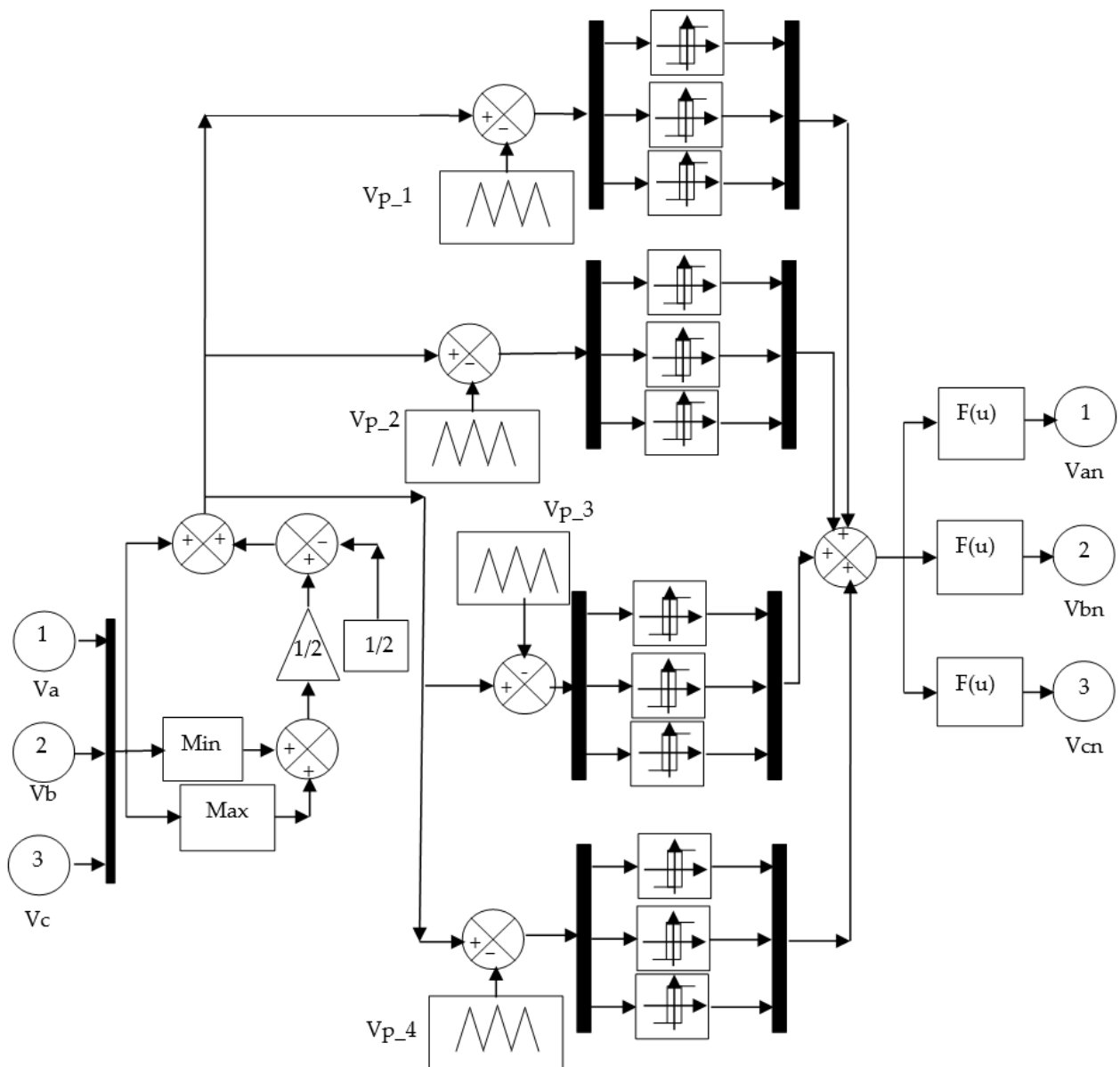


Figure 4. Structure of the five-level SVM technique.

The internal form of the FLA method is shown in Figure 6. From this figure, it is noted that the structure of the FLA technique is simple. This fuzzy controller has two inputs, the error and the change in error, and only one output. Three constant gains (K_1 , K_2 , and K_3) are used to improve the response and adjust the response of fuzzy logic. The characteristics of the FLA method used to improve the performance and effectiveness of the proposed five-level SVM technique are shown in the bottom of the Figure 6. The type of fuzzy controller used in this work is the Mamdani controller.

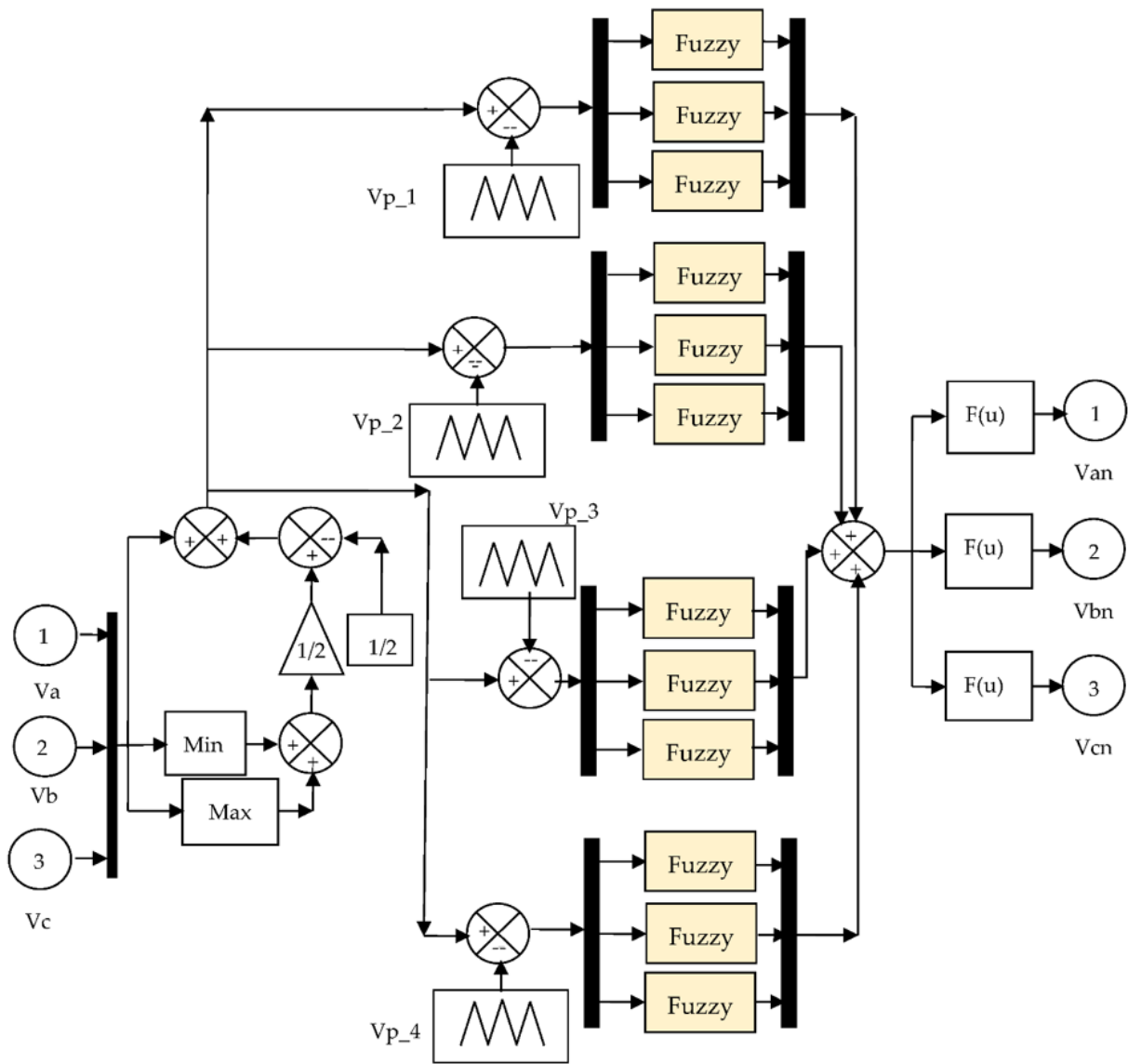
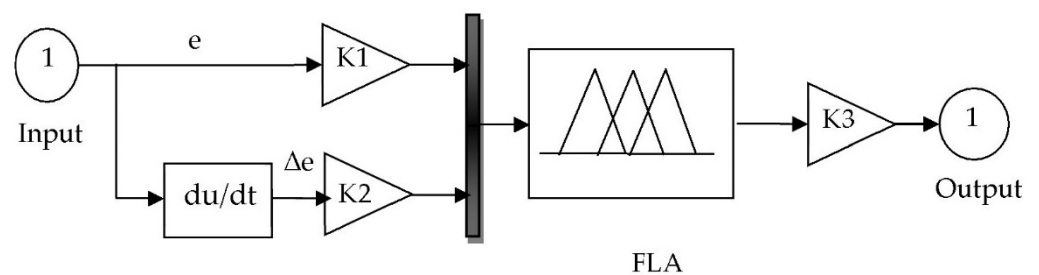


Figure 5. Structure of the proposed five-level fuzzy SVM technique.



Parameters of the FLA

Or method	Max
And method	Min
Fis type	Mamdani
Defuzzification	Centroid
Implication	Min
Aggregation	Max

Figure 6. Structure and parameters of the fuzzy logic technique.

Seven membership functions (MFs) are used in the first entry (error) and seven MFs are used in the second input (change in error). These functions used to accomplish fuzzy logic are shown in Figure 7a,b. In order to get a good response and results for the fuzzy logic, the 7×7 rule is used, where these rules are represented in Figure 7c.

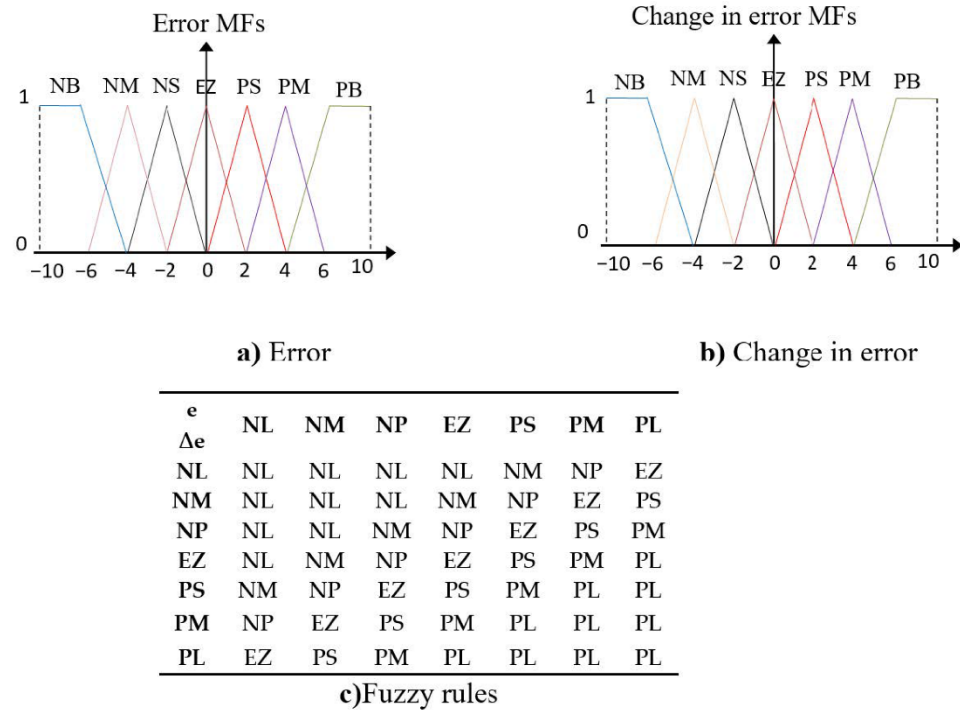


Figure 7. Membership functions and fuzzy rules.

Using the Matlab/Simulink software, the surface for the fuzzy logic controller used in this paper is given in order to compensate for the traditional hysteresis comparators. This surface of the fuzzy logic controller is shown in Figure 8. The use of the fuzzy logic technique leads to improving the performance and effectiveness of the proposed five-level SVM technique and thus obtaining a good quality of the electric current, and this is the main objective of this work.

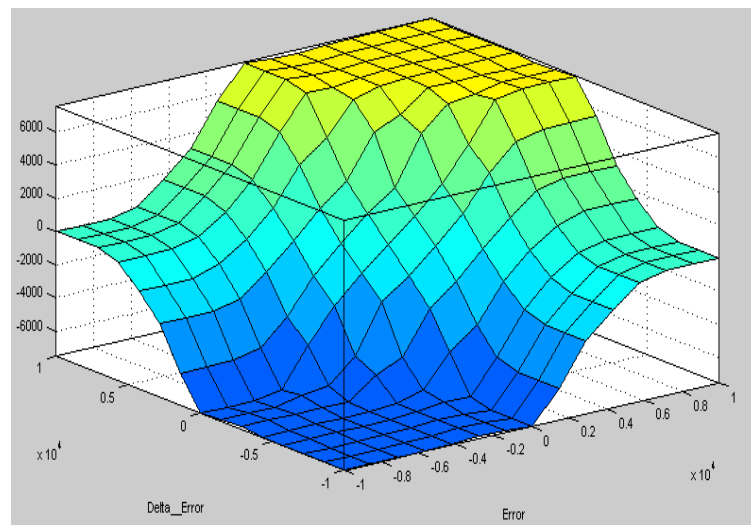


Figure 8. Control surface.

Compared to the PWM technique, the proposed five-level fuzzy SVM (FSVM) method is more complex and contains 12 fuzzy logic controllers which make it not easy and costly compared to the traditional PWM technique. However, in terms of the results obtained, the proposed method is better than the PWM technique. The proposed five-level fuzzy SVM method gives the output of the inverter a high-quality electrical signal (current) with a small value of THD.

5. Traditional IFOC Strategy

The IFOC method is a type of FOC method which offers a fast dynamic response compared to the direct FOC method [28]. The indirect FOC method is a method that differs from the direct FOC method in terms of the principle of work and in terms of internal structure. Several scientific works dealt with this method [29–31], where four PI controllers are used in this method, which makes the dynamic response much faster. Thus, the indirect FOC method is more complex than the direct FOC method [32], but the indirect FOC method provides a better dynamic response than the direct FOC method. Moreover, the indirect FOC method reduces the ripples of torque, reactive power, and flux compared to the direct FOC method [33]. In order to control the generator inverter, the PWM technique is used. This method is based on the principle shown in Equation (21) [34].

$$\Psi_{qs} = 0 \text{ and } \Psi_{ds} = \Psi_s \quad (21)$$

Using Equation (21), the direct and quadrature stator voltages of the generator become as follows:

$$\begin{cases} V_{ds} = V_s = \omega_s \Psi_s \\ V_{qs} = 0 \end{cases} \quad (22)$$

Using Equations (13) and (22), the direct and quadrature stator currents of the generator become as follows:

$$\begin{cases} I_{ds} = -\frac{M}{L_s} I_{dr} + \frac{\Psi_s}{L_s} \\ I_{qs} = -\frac{M}{L_s} I_{qr} \end{cases} \quad (23)$$

Relying on Equations (11) and (23), the direct and indirect rotor voltages of the generator become as follows [34]:

$$\begin{cases} V_{qr} = R_{dr} I_{qr} + \left(L_r - \frac{M^2}{L_s} \right) \omega_r I_{qr} + g \frac{M V_s}{L_s} \\ V_{dr} = R_{dr} I_{dr} - \omega_r \left(L_r - \frac{M^2}{L_s} \right) I_{qr} \end{cases} \quad (24)$$

The direct and quadrature rotor flux of a generator can be expressed by the following equation [33]:

$$\begin{cases} \Psi_{dr} = \left(L_r - \frac{M^2}{L_s} \right) I_{dr} + \frac{M}{\omega_s L_s} V_s \\ \Psi_{qr} = \left(L_r - \frac{M^2}{L_s} \right) I_{qr} \end{cases} \quad (25)$$

By Equation (25), direct rotor flux is related to both stator voltage and quadrature rotor current. As for the quadrature rotor flux, it is related to the quadrature rotor current of the generator.

From Equations (21)–(25), the internal structure of the indirect FOC strategy can be given in Figure 9. Through this figure, we note that this technique controls the reactive and active power by controlling the quadrature and direct rotor voltages (V_{qr}^* and V_{dr}^*).

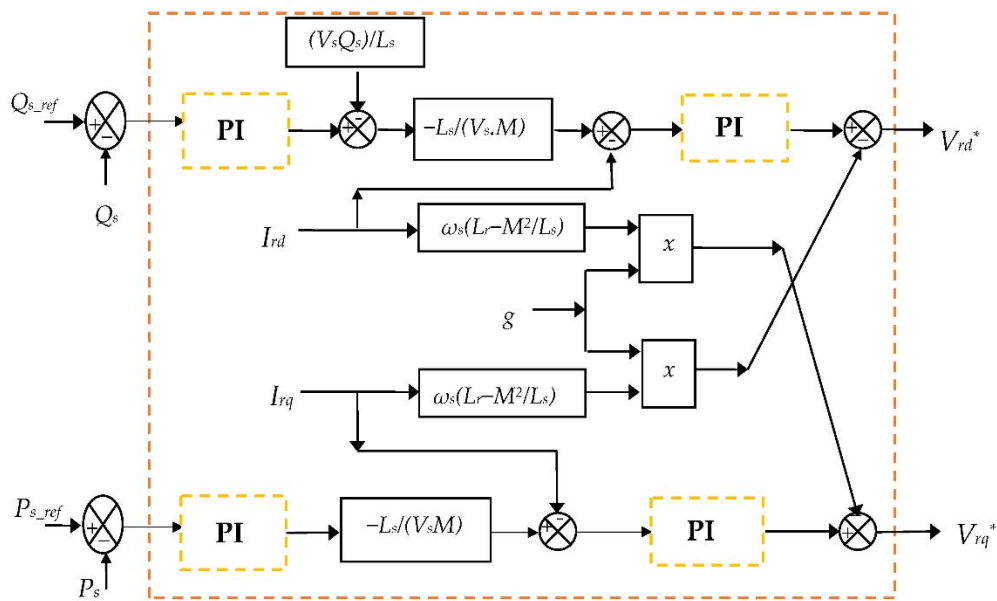


Figure 9. Traditional indirect FOC strategy.

In order to estimate the active and reactive power, Equation (26) is used. In order to estimate the two values, we need to measure both rotor voltage and rotor current.

$$\begin{cases} Q_s = -1.5 \left(\frac{\omega_s \Psi_s M}{L_s} I_{dr} - \frac{\omega_s \Psi_s^2}{L_s} \right) \\ P_s = -1.5 \frac{\omega_s \Psi_s M}{L_s} I_{qr} \end{cases} \quad (26)$$

Figure 10 represents the total system used in this paper, where a multi-rotor wind turbine (MRWT) was used to rotate the generator (DPIG). The latter is controlled by the traditional IFOC method. In this work, the reference value of the reactive power (Q_s^*) is set to 0 Var. The reference value of the active power (P_s^*) is obtained using the MPPT technique.

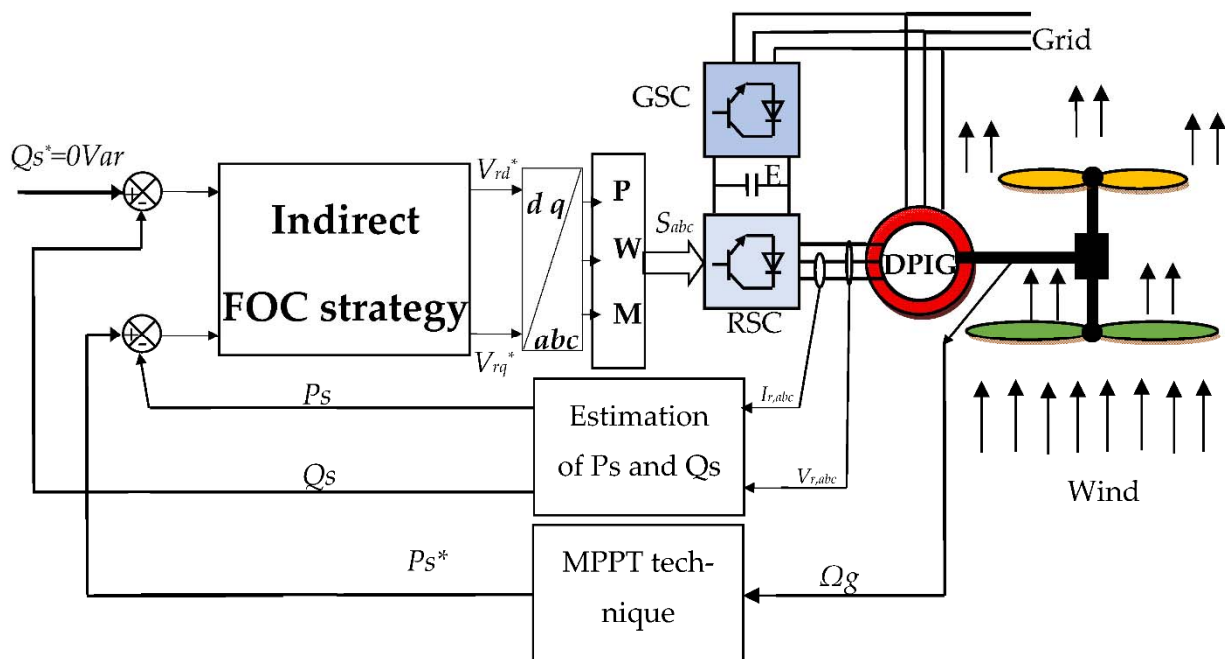


Figure 10. Traditional IFOC technique of the DPIG-based MRWT system.

The indirect FOC strategy gives more ripples in the current, torque, active power, and flux compared to DPC and DTC. Moreover, it has a long dynamic response and gives a poor quality of electric current and active power.

The reason for these shortcomings in this traditional indirect FOC strategy is due to the use of both the traditional PWM technique and conventional PI controller. The use of these classic methods (PI and PWM) makes the indirect FOC strategy not robust and characterized by a long dynamic response compared to some methods such as the DTC strategy.

In order to improve the performance and efficacy of the traditional indirect FOC strategy, a novel scheme for the traditional indirect FOC strategy is proposed in Section 6. This proposed indirect FOC strategy is based on the use of both the proposed SSTA algorithm and the multilevel fuzzy SVM strategy.

6. Proposed Indirect FOC Strategy

In this part, a new idea for indirect FOC strategy is presented based on the proposed simplified STA controller and the five-level fuzzy SVM strategy. The proposed indirect FOC method is a change from the classic indirect FOC method, where the proposed SSTA controller is used in place of the traditional PI controller and the five-level fuzzy SVM technique is used instead of the PWM technique. This proposed indirect FOC method aims to control the active and reactive power of the generator placed in the multi-rotor wind turbine system. On the other hand, this proposed indirect FOC method reduces the ripples of torque, active power, and electric current compared to the classical indirect FOC method. The proposed indirect FOC strategy is shown in Figure 11. From this figure, to control the active/reactive power, two proposed SSTA controllers are used and the same with the reactive power.

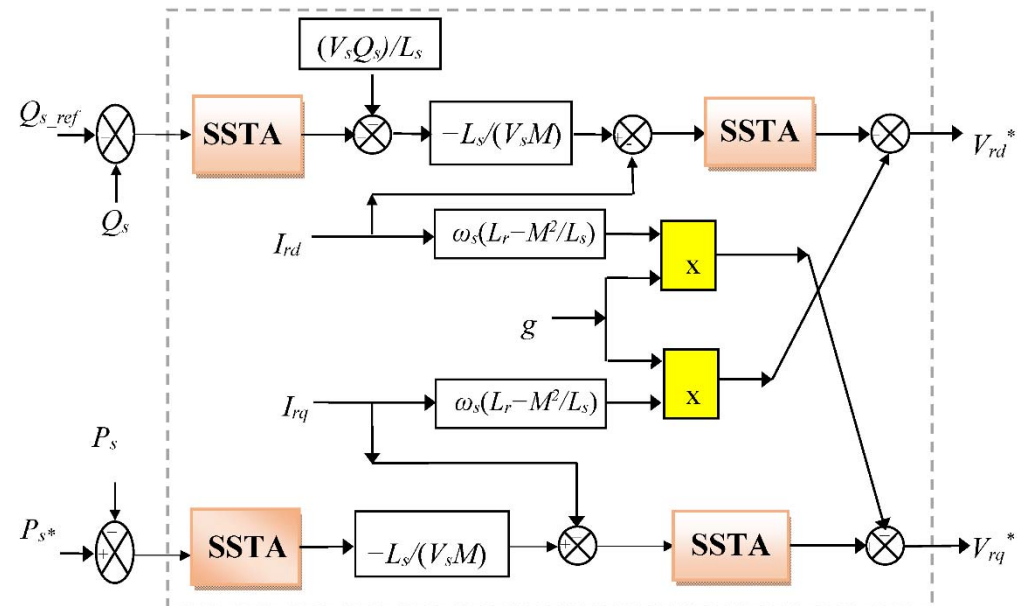


Figure 11. Proposed indirect FOC strategy.

In this proposed indirect FOC method, the same equations used to estimate both the active and reactive power are used in the classical indirect FOC strategy. Therefore, it can be said that this designed indirect FOC strategy is more robust than the rest of the controls such as the classical indirect FOC strategy and DTC. The objective of this designed indirect FOC strategy is to obtain high-quality V_{qr}^* and V_{dr}^* from active and reactive power references for the inverter DFIG control. Controlling the latter very well leads to obtaining a high quality of stator current and active power. On the other hand, the reactive power reference is set to zero. As for the reference value of the active power, it is obtained using

the maximum power point tracking (MPPT) technique. The system studied using the proposed indirect FOC method is represented in Figure 12, where almost the same structure as the classical indirect FOC method is preserved.

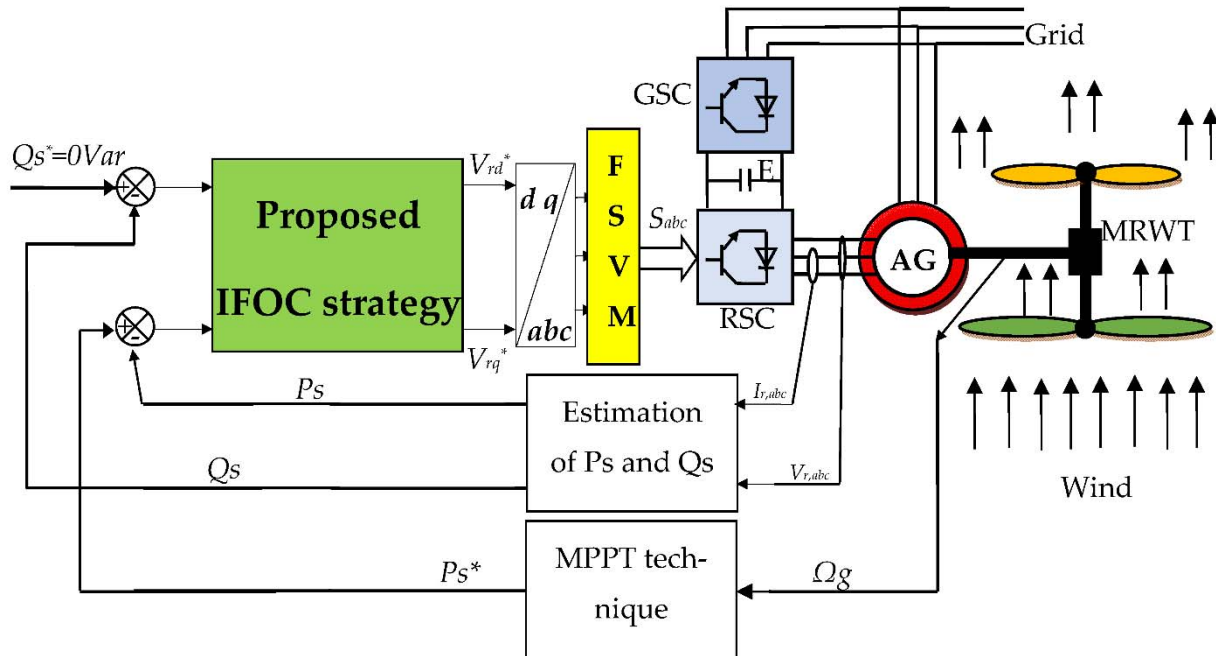


Figure 12. Proposed indirect FOC strategy of DPIG-based MRWT system.

In Table 1, a comparison is given between the classical indirect FOC (IFOC) technique and the proposed indirect FOC method. Through this table, the proposed indirect FOC strategy is more robust and reduces torque and current ripples compared to the classical indirect FOC technique. Moreover, the proposed indirect FOC method improves the rise time, response dynamic, THD value of current, and power quality compared to the classical indirect FOC technique. However, the proposed indirect FOC method is more complicated than the classical indirect FOC method due to the use of the five-level fuzzy SVM (FSVM) technique (instead, the classical indirect FOC method uses the PWM technique).

Table 1. A comparative study between the classical method and the proposed IFOC strategy.

	Traditional Indirect FOC Technique	Proposed Indirect FOC Technique
Type controller used	PI controller	SSTA controller
Rise time	High	Low
Modulation	PWM	Fuzzy SVM
Degree of complexity	Medium	High
Ease	Medium	Complicated
Simplicity of implementation	Medium	Complicated
Response dynamic	Slow	Quick
Robustness	Low	High
THD	High	Low
Power ripple	High	Low

The result of using the five-level fuzzy SVM technique in the proposed IFOC method makes the proposed IFOC method not simple and somewhat complicated compared to the classical IFOC method, where the latter uses PWM, which leads to problems in the case of achieving this proposed IFOC-SSTA-FSVM method.

To implement the proposed method (IFOC-SSTA-FSVM) empirically, there are several problems of implementation related to the large financial cost of completing this project

due to the complexity of controlling the MRWT system. On the other hand, there is the complexity of the use of the five-level fuzzy SVM technique to control the inverter of the DFIG-based MRWT system. Moreover, the use of the maximum power point tracking technique increases the complexity and financial cost of the studied MRWT system. Nonetheless, given the results obtained in improving the quality of electric power and the importance of the MRWT system in improving the performance of classical wind turbines and in reducing the size of wind farms, this system is very necessary for the near future.

In the next part, the results are confirmed and the robustness of the proposed indirect FOC method is verified using the Matlab/Simulink software.

7. Results

In order to verify the proposed indirect FOC method, the Matlab/Simulink software is used. The results of the proposed indirect FOC method are compared with the classical indirect FOC method in terms of the ratio of ripples at the level of torque, current, effective power, and reactive power. The two methods are also compared in terms of the THD value of the electric current.

In this work, a generator with the following data is used: 50 Hz, 380/696 V, $R_s = 0.012 \Omega$, $L_r = 0.0136$ H, $L_m = 0.0135$ H, $p = 2$, $J = 1000$ kg·m², $P_{sn} = 1.5$ MW, $R_r = 0.021 \Omega$, $L_s = 0.0137$ H, and $f_r = 0.0024$ N·m/s [35].

In this work, a multi-rotor wind turbine with the following data is used: $R_1 = 13.2$ m, $R_2 = 25.5$ m, $r_1 = 1$ m, $r_2 = 0.5$ m, $r_g = 0.75$ m, $J_1 = 500$ kg·m², $J_2 = 1000$ kg·m², $G_1 = r_1/r_g$, and $G_2 = r_2/r_g$.

In this work, the proposed indirect FOC method is tested in the case of two tests, the first test is a tracking test and the second test is to study the behavior of the proposed indirect FOC method in comparison with the classical indirect FOC method in the event of a change in the generator parameters. This is in order to know the robustness of the proposed indirect FOC method with the classical indirect FOC method.

7.1. First Test

In this test, the behavior of the reference tracking is studied, for both the proposed IFOC-SSTA method and the classical IFOC method, where the obtained results are shown in Figure 13. Through this figure, the active and reactive power follow the references perfectly, and this is for the two IFOC methods with a preference for the proposed method in the dynamic response (see Figure 13a,b). The proposed IFOC-SSTA method gave better results in terms of ripples for both active and reactive power compared to the classical IFOC method (see Figure 14a,b). In Figure 13c, the generated torque has the same shape as the active power, where it can be seen that the increase in the active power corresponds to the increase in the torque. In addition, the proposed IFOC-SSTA method reduced torque ripples compared to the classical IFOC method (Figure 14c).

Regarding the current generated by the generator, it is shown in Figure 15d. Through this figure, the electric current takes the form of the active power, where it is noted that the behavior of the current is the same as the behavior of the active power. Moreover, the proposed IFOC-SSTA method gave excellent results in terms of electric current ripples and quality compared to the classical IFOC method (see Figure 14d).

Figure 13e,f represent the THD value of the proposed and classical IFOC method, respectively. Through these two forms, the proposed IFOC-SSTA method reduced the THD value of the electric current excellently compared to the classical IFOC method and the reduction ratio was about 96.72%. These results confirm the robustness of the proposed IFOC method in improving the quality of the effective power and electric current.

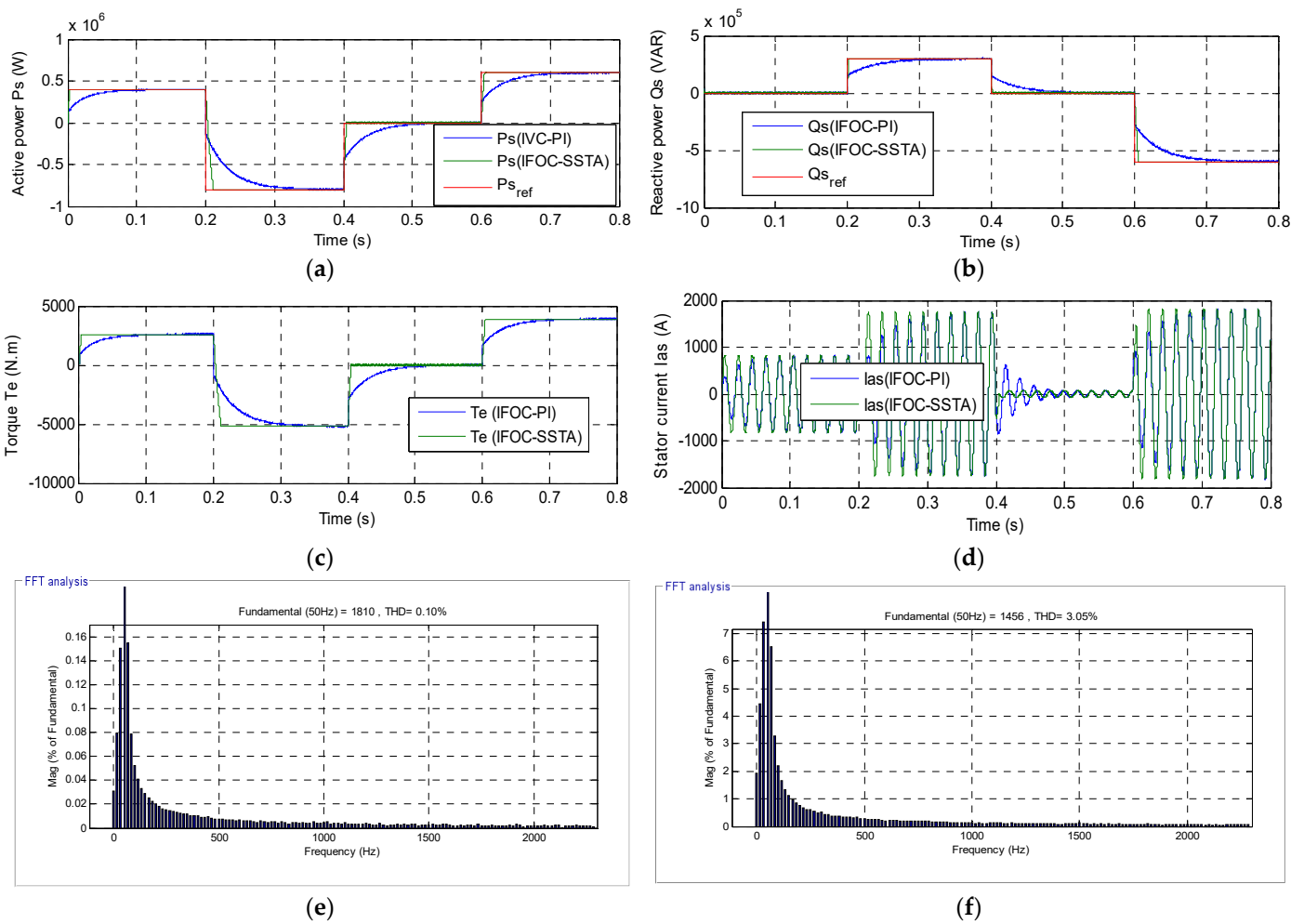


Figure 13. First test results. (a) Active power; (b) Reactive power; (c) Torque; (d) Stator current; (e) THD value of stator current (IFOC-SSTA strategy); (f) THD value of stator current (IFOC strategy).

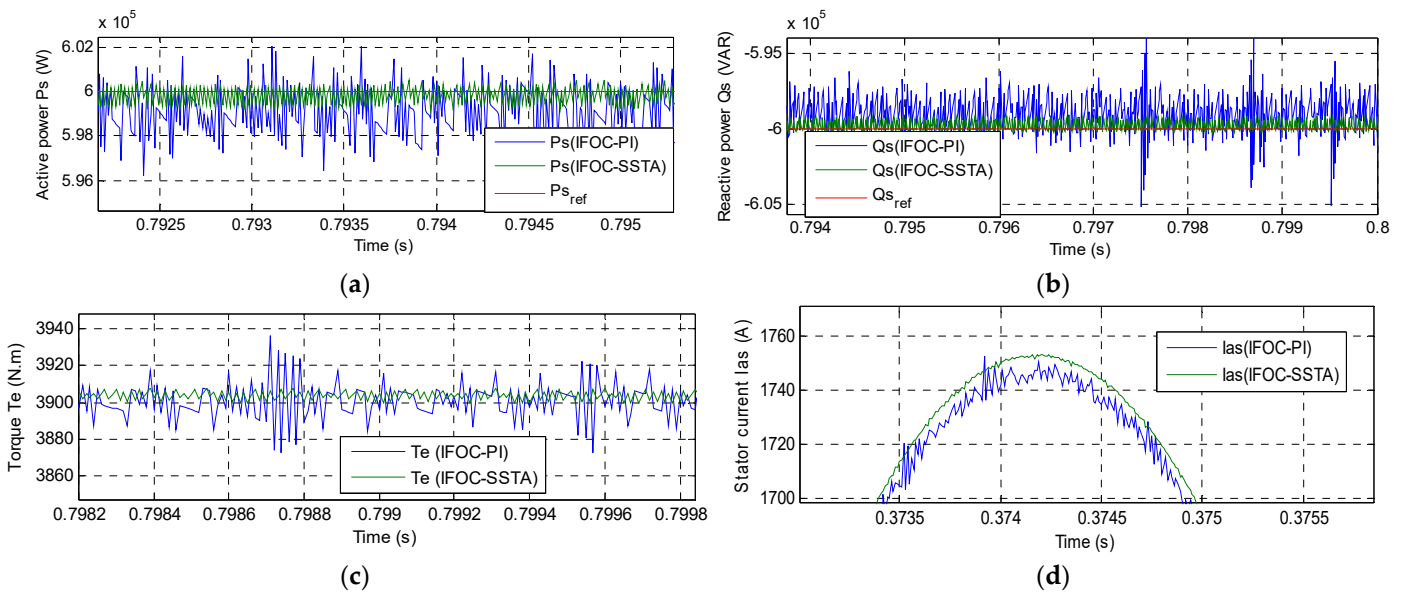


Figure 14. Zoom in the first test results. (a) Active power; (b) Reactive power; (c) Torque; (d) Stator current.

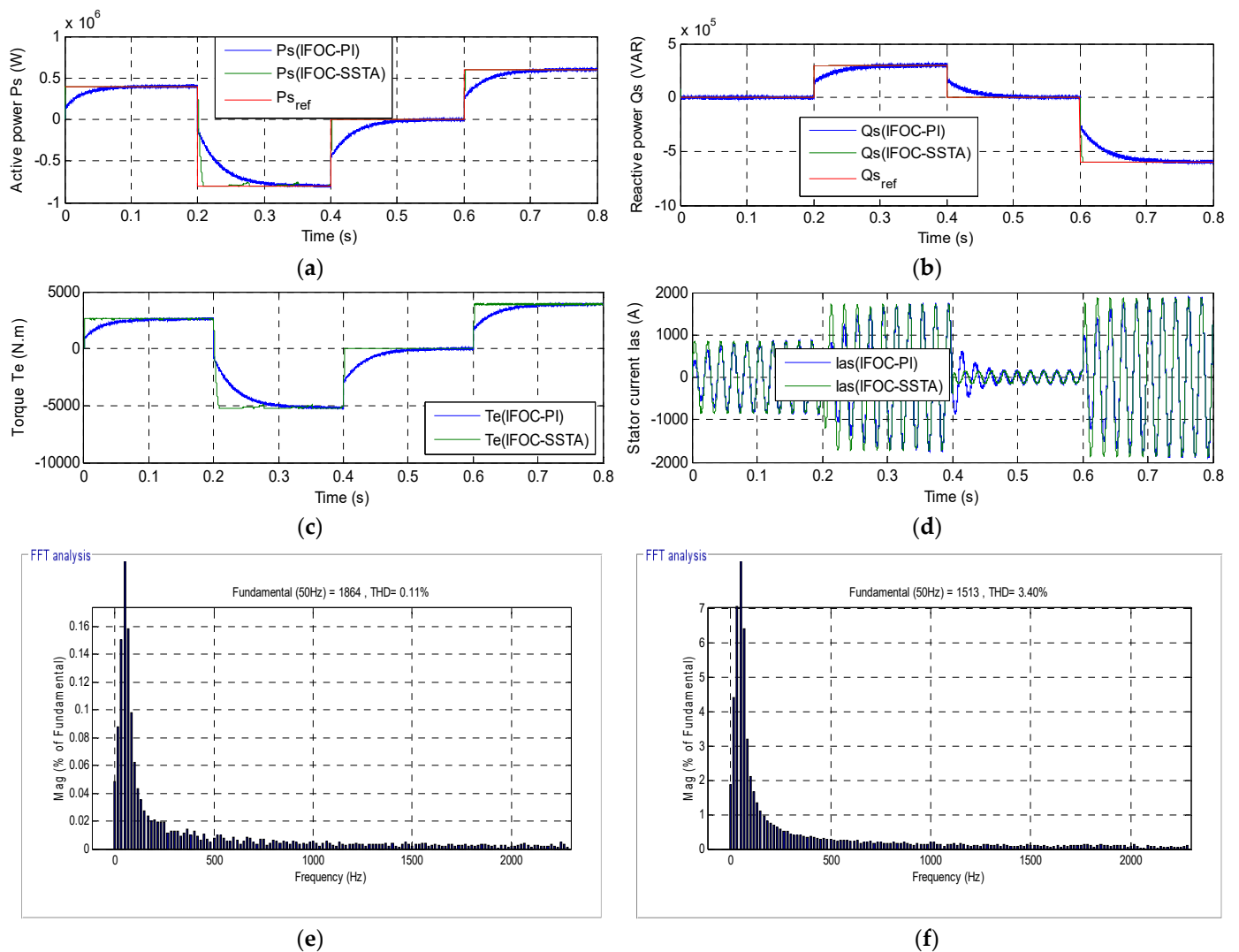


Figure 15. Second test results. (a) Active power; (b) Reactive power; (c) Torque; (d) Stator current; (e) THD value of current (IFOC-SSTA strategy); (f) THD value of current (IFOC strategy).

In the next test, the proposed IFOC method is further confirmed if the parameters of the generator installed in the multi-rotor wind turbine system are changed.

The results obtained from this test are shown in Table 2. Table 2 represents the value of ripples in each of torque, current, active power, and reactive power, and this is for the two IFOC methods. Through this table, the proposed IFOC-SSTA method reduced the ratio of ripples of torque, active power, current, and reactive power by excellent ratios, and the ratios were as follows: 91.66%, 91.20%, 84.21%, and 93.75%, respectively.

Table 2. Comparative ripples obtained from the traditional IFOC with the proposed IFOC strategy.

	Classical IFOC Technique	Proposed IFOC Technique	Ratios
Torque ripple (N.m)	Around 60	Around 5	91.66%
Reactive power ripple (VAR)	Around 8000	Around 500	93.75%
Active power ripple (W)	Around 10,000	Around 880	91.20%
Stator current (A)	Around 19	Around 3	84.21%

In Table 3, the response time is extracted for each of the active power, torque, and reactive power of the two IFOC methods proposed in this work. Through this table, the proposed IFOC-SSTA method gave a small response time compared to the classical IFOC

method, and the improvement ratio was about 97.54%, 97.54%, and 98.23% for the active power, torque, and reactive power, respectively. Moreover, the proposed method gave a good response time in comparison with both the DPC strategy and neuro-second order sliding mode control (NSOSMC) completed in [36] (see Table 4).

Table 3. Response time.

	Response Time		
	Torque	Reactive Power	Active Power
Classical IFOC strategy	0.12 s	0.13 s	0.12 s
Proposed IFOC strategy	2.95 ms	0.0023 s	2.95 ms
Ratios	97.54%	98.23%	97.54%

Table 4. Comparative analysis of response time.

	Response Time		
	Torque	Reactive Power	Active Power
Proposed technique: IFOC-SSTA	2.95 ms	0.0023 s	2.95 ms
[36] Direct power control	18 ms	17 ms	18 ms
Neuro-second order SMC technique	5 ms	9 ms	5 ms

7.2. Second Test

The results of the second test are shown in Figure 15. In this test, the generated parameter values were changed in order to know the change in the behavior of the proposed IFOC-SSTA method compared to the classical IFOC method, as well as its robustness. In this test, R_s , L_s , R_r , L_m , and L_r were changed to the values 0.024 Ω , 0.00685 H, 0.042 Ω , 0.00675 H, and 0.0068 H, respectively. Zoom is given for torque, current, effective power, and reactive power in Figure 16. In Figures 15 and 16, there is a noticeable effect on the level of torque, current, active, and reactive power, where the classical IFOC method was affected by changing the generator parameters more than the IFOC-SSTA method. Moreover, active and reactive power keep following the references well in this test for both the proposed and the classical IFOC method (see Figure 15a,b). Both current and torque take the same form as active power (see Figure 15c,d) with ripples in both torque and current levels. The proposed IFOC-SSTA method reduced these ripples as compared to the classical IFOC method (see Figure 16c,d). Moreover, the proposed IFOC-SSTA method also reduced the ripples in both the active and reactive power compared to the classical IFOC method (see Figure 16a,b). The THD value of the electric current is shown in Figure 15e,f and this is for both the proposed and the classical IFOC method, respectively. Through the two figures, the proposed IFOC-SSTA method reduced the THD value of the electric current compared with the classical IFOC method.

The results obtained from this test are shown in Table 5. Through this table, the proposed IFOC-SSTA method reduced the ripples of torque, reactive power, current, and active power by 93.35%, 98%, 87.50%, and 83.33%, respectively.

The proposed IFOC-SSTA-FSVM method in this work provided excellent results compared to the classical IFOC method in terms of reducing the ripples of torque, current, and active power, as well as improving the quality of electric power. All of these factors help reduce malfunctions and thus reduce maintenance costs and help extend the life of the system as a whole.

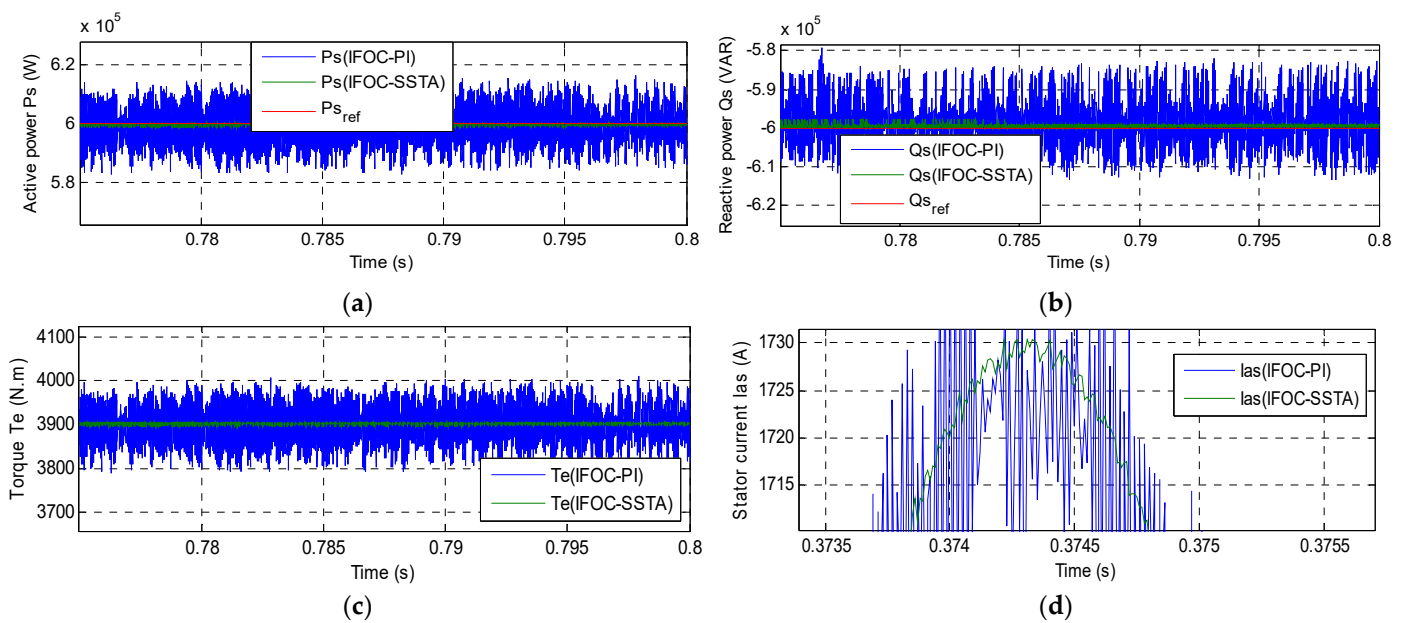


Figure 16. Zoom in the second test results. (a) Active power; (b) Reactive power; (c) Torque; (d) Stator current.

Table 5. Comparative ripples obtained from both techniques.

	Traditional IFOC Strategy	Designed IFOC Technique	Ratios
Torque ripple (N.m)	Around 172	Around 11.60	93.35%
Reactive power ripple (VAR)	Around 25,000	Around 500	98%
Active power ripple (W)	Around 30,000	Around 5000	83.33%
Stator current (A)	Around 40	Around 5	87.50%

The following is a comparison between the proposed IFOC-SSTA-FSVM method and some published works in terms of the THD value of the electric current. The results of the comparison are recorded in Table 6. Through this table, the proposed IFOC-SSTA-FSVM method significantly reduced the THD value compared to several published methods, which indicates the robustness of the proposed IFOC-SSTA-FSVM method and the effectiveness of the proposed IFOC-SSTA-FSVM method in improving the quality of electrical energy.

Table 6. Comparative results with other techniques.

References	Techniques	THD (%)
[37]	Field-oriented control with PI controllers	0.77
	Super twisting algorithm (STA)	0.28
[38]	Fuzzy DTC strategy	2.40
[39]	Fractional-order sliding mode control	1.31
	Integral SMC technique	9.71
[40]	Multi-resonant-based sliding mode controller (MRSMC)	3.14
[41]	Backstepping control	2.19
[6]	Field-oriented control	3.7
	DPC control with PI controllers	0.46
[12]	DPC control with terminal synergetic controllers	0.25
[42]	Direct torque control with second-order continuous SMC technique	0.78
[28]	DPC control with integral-proportional controllers	0.43
	DFOC control with PI controllers	1.45
[9]	DFOC control with synergetic-SMC technique	0.50

Table 6. Cont.

References	Techniques	THD (%)
[13]	Field-oriented control with neuro-fuzzy controller	0.78
[43]	Field-oriented control with type-2 fuzzy logic controllers	1.14
[32]	Multilevel DTC strategy	1.57
[44]	Vector control	2.20
[45]	Adaptive backstepping sliding mode control	1.15
[44]	Traditional direct vector control	1.65
[45]	DPC with sliding mode controller	1.66
Proposed IFOC strategy	DPC with super twisting sliding mode controller	0.11
	First test	0.10
	Second test	0.11

8. Conclusions

In this work, a new idea was given for the IFOC method based on both a simplified STA controller and a five-level fuzzy SVM technique. This proposed method was verified using the Matlab/Simulink software, comparing the results obtained with the traditional method. The application of the proposed method in the wind system led to the improvement of the dynamic response of the generator and the improvement of the quality of the electric current with the electric energy.

The points drawn from this work are illustrated in the following points:

- A new fuzzy SVM technology was introduced to control the five-level inverter to give a constant frequency at the inverter output, with this method confirmed by numerical simulation.
- A new simplified STA controller was proposed in this paper.
- A new indirect FOC strategy based on the simplified STA controller and the proposed five-level fuzzy SVM technique was presented and confirmed with numerical simulation.
- The robustness of the proposed indirect FOC strategy was presented.
- The characteristics of the designed indirect FOC strategy was analyzed, showing that the undulations of the reactive power, stator current, torque, and active power were minimized.

In a future paper, to ameliorate the quality of the active power and current, the DPIG will be controlled using another robust control scheme, such as fractional order synergetic control and feedback PI controller [46,47].

Author Contributions: Validation, N.B., P.T. and N.T.; conceptualization, H.B.; software, H.B.; methodology, H.B.; investigation, H.B. and I.C.; resources, N.B., P.T. and N.T.; project administration, N.B.; data curation, N.B., P.T. and N.T.; writing—original draft preparation, H.B.; supervision, N.B. and I.C.; visualization: I.C. and N.B.; formal analysis: I.C. and N.B.; funding acquisition: N.B., P.T. and N.T.; writing—review and editing: I.C., N.B., P.T., N.T. and H.B. All authors have read and agreed to the published version of the manuscript.

Funding: This work was supported in part by the Framework Agreement between University of Pitesti (Romania) and King Mongkut's University of Technology North Bangkok (Thailand), in part by an International Research Partnership "Electrical Engineering–Thai French Research Center (EE-TFRC)" under the project framework of the Lorraine Université d'Excellence (LUE) in cooperation between Université de Lorraine and King Mongkut's University of Technology North Bangkok, in part by the National Research Council of Thailand (NRCT) under Senior Research Scholar Program under Grant No. N42A640328, and in part by National Science, Research, and Innovation Fund (NSRF) under King Mongkut's University of Technology North Bangkok under Grant no. KMUTNB-FF-65-20.

Institutional Review Board Statement: Not applicable.

Informed Consent Statement: Not applicable.

Data Availability Statement: Not applicable.

Conflicts of Interest: The authors declare no conflict of interest.

References

1. Mohamed Ahmed, S.A.; Montaser Abd El Sattar, M.A. Dynamic Performance and Effectiveness of Voltage Disturbances on the Improvement of Power Quality for Grid-Connected DFIG System Based Wind Farm. *J. Electr. Eng. Electron. Control. Comput. Sci.* **2020**, *5*, 25–30. Available online: <https://jeeeccs.net/index.php/journal/article/view/126> (accessed on 9 April 2022).
2. Talla, J.; Leu, V.Q.; Šmídl, V.; Peroutka, Z. Adaptive Speed Control of Induction Motor Drive With Inaccurate Model. *IEEE Trans. Ind. Electron.* **2018**, *65*, 8532–8542. [[CrossRef](#)]
3. Wolkiewicz, M.; Tarchała, G.; Orłowska-Kowalska, T.; Kowalski, C.T. Online Stator Interturn Short Circuits Monitoring in the DFOC Induction-Motor Drive. *IEEE Trans. Ind. Electron.* **2016**, *63*, 2517–2528. [[CrossRef](#)]
4. Candelo-Zuluaga, C.; Riba, J.-R.; Garcia, A. PMSM Parameter Estimation for Sensorless FOC Based on Differential Power Factor. *IEEE Trans. Instrum. Meas.* **2021**, *70*, 1–12. [[CrossRef](#)]
5. Alexandrou, A.D.; Adamopoulos, N.K.; Kladas, A.G. Development of a Constant Switching Frequency Deadbeat Predictive Control Technique for Field-Oriented Synchronous Permanent-Magnet Motor Drive. *IEEE Trans. Ind. Electron.* **2016**, *63*, 5167–5175. [[CrossRef](#)]
6. Amrane, F.; Chaiba, A.; Babes, B.E.; Mekhilef, S. Design and implementation of high performance field oriented control for grid-connected doubly fed induction generator via hysteresis rotor current controller. *Rev. Roum. Sci. Tech.-Electrotech. Energ* **2016**, *61*, 319–324.
7. Eltamaly, A.M.; Al-Saud, M.; Sayed, K.; Abo-Khalil, A.G. Sensorless active and reactive control for DFIG wind turbines using opposition-based learning technique. *Sustainability* **2020**, *12*, 3583. [[CrossRef](#)]
8. Habib, B.; Lemdani, S. Combining synergetic control and super twisting algorithm to reduce the active power undulations of doubly fed induction generator for dual-rotor wind turbine system. *Electr. Eng. Electromech.* **2021**, *2021*, 8–17.
9. Benbouhenni, H.; Bizon, N. A Synergetic Sliding Mode Controller Applied to Direct Field-Oriented Control of Induction Generator-Based Variable Speed Dual-Rotor Wind Turbines. *Energies* **2021**, *14*, 4437. [[CrossRef](#)]
10. Habib, B. Application of STA methods and modified SVM strategy in direct vector control system of ASG integrated to dual-rotor wind power: Simulation studies. *Int. J. Smart Grid* **2021**, *5*, 62–72.
11. Habib, B. Amelioration effectiveness of torque and rotor flux control applied to the asynchronous generator (AG) for dual-rotor wind turbine using neural third-order sliding mode approaches. *Int. J. Eng. Trans. C: Asp.* **2022**, *35*, 517–530.
12. Benbouhenni, H.; Bizon, N. Terminal Synergetic Control for Direct Active and Reactive Powers in Asynchronous Generator-Based Dual-Rotor Wind Power Systems. *Electronics* **2021**, *10*, 1880. [[CrossRef](#)]
13. Amrane, F.; Chaiba, A. A novel direct power control for grid-connected doubly fed induction generator based on hybrid artificial intelligent control with space vector modulation. *Rev. Sci. Tech.-Electrotech. Et Energ.* **2016**, *61*, 263–268.
14. Brando, G.; Dannier, A.; Spina, I. Performance Analysis of a Full Order Sensorless Control Adaptive Observer for Doubly-Fed Induction Generator in Grid Connected Operation. *Energies* **2021**, *14*, 1254. [[CrossRef](#)]
15. Yahdou, A.; Hemici, B.; Boudjema, Z. Second order sliding mode control of a dual-rotor wind turbine system by employing a matrix converter. *J. Electr. Eng.* **2016**, *16*, 1–11.
16. Erturk, E.; Sivrioglu, S.; Bolat, F.C. Analysis Model of a Small Scale Counter-Rotating Dual Rotor Wind Turbine with Double Rotational Generator Armature. *Int. J. Renew. Energy Res.* **2018**, *8*, 1849–1858.
17. Fukami, T.; Momiyama, M.; Shima, K.; Hanaoka, R.; Takata, S. Steady-State Analysis of a Dual-Winding Reluctance Generator With a Multiple-Barrier Rotor. *IEEE Trans. Energy Convers.* **2008**, *23*, 492–498. [[CrossRef](#)]
18. Worku, M.Y.; Hassan, M.A.; Abido, M.A. Real Time-Based under Frequency Control and Energy Management of Microgrids. *Electronics* **2020**, *9*, 1487. [[CrossRef](#)]
19. Wang, L.; Kerrouche, K.D.E.; Mezouar, A.; Van Den Bossche, A.; Draou, A.; Boumediene, L. Feasibility Study of Wind Farm Grid-Connected Project in Algeria under Grid Fault Conditions Using D-Facts Devices. *Appl. Sci.* **2018**, *8*, 2250. [[CrossRef](#)]
20. Han, Y.; Ma, R. Adaptive-Gain Second-Order Sliding Mode Direct Power Control for Wind-Turbine-Driven DFIG under Balanced and Unbalanced Grid Voltage. *Energies* **2019**, *12*, 3886. [[CrossRef](#)]
21. Alhato, M.M.; Ibrahim, M.N.; Rezk, H.; Bouallègue, S. An Enhanced DC-Link Voltage Response for Wind-Driven Doubly Fed Induction Generator Using Adaptive Fuzzy Extended State Observer and Sliding Mode Control. *Mathematics* **2021**, *9*, 963. [[CrossRef](#)]
22. Alhato, M.M.; Bouallègue, S.; Rezk, H. Modeling and Performance Improvement of Direct Power Control of Doubly-Fed Induction Generator Based Wind Turbine through Second-Order Sliding Mode Control Approach. *Mathematics* **2020**, *8*, 2012. [[CrossRef](#)]
23. Djilali, L.; Badillo-Olvera, A.; Rios, Y.Y.; López-Beltrán, H.; Saihi, L. Neural High Order Sliding Mode Control for Doubly Fed Induction Generator based Wind Turbines. *IEEE Lat. Am. Trans.* **2022**, *20*, 223–232. [[CrossRef](#)]
24. Halabi, L.M.; Alsofyani, I.M.; Lee, K.-B. Multi Open-/Short-Circuit Fault-Tolerance Using Modified SVM Technique for Three-Level HANPC Converters. *IEEE Trans. Power Electron.* **2021**, *36*, 13621–13633. [[CrossRef](#)]
25. Habib, B. Utilization of an ANFIS-STSM algorithm to minimize total harmonic distortion. *Int. J. Smart Grid* **2020**, *4*, 56–67.

26. Habib, B.; Boudjema, Z.; Belaidi, A. Direct power control with NSTSM algorithm for DFIG using SVPWM technique. *Iranian J. Electr. Electron. Eng.* **2021**, *17*, 1–11.
27. Habib, B.; Boudjema, Z.; Belaidi, A. Neuro-second order sliding mode control of a DFIG supplied by a two-level NSVM inverter for wind turbine system. *Iran. J. Electr. Electron. Eng.* **2018**, *14*, 362–373.
28. Fayssal, A.; Bruno, F.; Azeddine, C. Experimental investigation of efficient and simple wind-turbine based on DFIG-direct power control using LCL-filter for stand-alone mode. *ISA Trans.* **2021**, 1–34, *in press*. [[CrossRef](#)]
29. Evangelista, C.; Valenciaga, F.; Puleston, P. Active and Reactive Power Control for Wind Turbine Based on a MIMO 2-Sliding Mode Algorithm With Variable Gains. *IEEE Trans. Energy Convers.* **2013**, *28*, 682–689. [[CrossRef](#)]
30. Habib, B.; Boudjema, Z.; Belaidi, A. Indirect vector control of a DFIG supplied by a two-level FSVM inverter for wind turbine system. *Majlesi J. Electr. Eng.* **2019**, *13*, 45–54.
31. Tang, Z.; Akin, B. A New LMS Algorithm Based Deadtime Compensation Method for PMSM FOC Drives. *IEEE Trans. Ind. Appl.* **2018**, *54*, 6472–6484. [[CrossRef](#)]
32. Yahdou, A.; Djilali, A.B.; Boudjema, Z.; Mehedi, F. Improved Vector Control of a Counter-Rotating Wind Turbine System Using Adaptive Backstepping Sliding Mode. *J. Eur. Des Systèmes Autom.* **2020**, *53*, 645–651. [[CrossRef](#)]
33. Boulaam, K.; Mekhilef, A. Output power control of a variable wind energy conversion system. *Rev. Sci. Techn.-Electrotech. Energ.* **2017**, *62*, 197–202.
34. Pan, L.; Zhu, Z.; Xiong, Y.; Shao, J. Integral Sliding Mode Control for Maximum Power Point Tracking in DFIG Based Floating Offshore Wind Turbine and Power to Gas. *Processes* **2021**, *9*, 1016. [[CrossRef](#)]
35. Yahdou, A.; Hemici, B.; Boudjema, Z. Sliding mode control of dual rotor wind turbine system. *Mediterr. J. Meas. Control* **2015**, *11*, 412–419.
36. Ibrahim, Y.; Semmah, A.; Patrice, W. Neuro-Second Order Sliding Mode Control of a DFIG based Wind Turbine System. *J. Electr. Electron. Eng.* **2020**, *13*, 63–68.
37. Hamid, C.; Aziz, D.; Eddine, C.S.; Othmane, Z.; Mohammed, T.; Hasnae, E. Integral sliding mode control for DFIG based WECS with MPPT based on artificial neural network under a real wind profile. *Energy Rep.* **2021**, *7*, 4809–4824. [[CrossRef](#)]
38. Ayrira, W.; Ourahoua, M.; El Hassounia, B.; Haddib, A. Direct torque control improvement of a variable speed DFIG based on a fuzzy inference system. *Math. Comput. Simul.* **2020**, *167*, 308–324. [[CrossRef](#)]
39. Beniss, M.A.; El Moussaoui, H.; Lamhamdi, T.; El Markhi, H. Improvement of power quality injected into the grid by using a FOSMC-DPC for doubly fed induction generator. *Int. J. Intell. Eng. Syst.* **2021**, *14*, 556–567. [[CrossRef](#)]
40. Quan, Y.; Hang, L.; He, Y.; Zhang, Y. Multi-Resonant-Based Sliding Mode Control of DFIG-Based Wind System under Unbalanced and Harmonic Network Conditions. *Appl. Sci.* **2019**, *9*, 1124. [[CrossRef](#)]
41. Zeghdi, Z.; Barazane, L.; Bekakra, Y.; Larbi, A. Improved backstepping control of a DFIG based wind energy conversion system using ant lion optimizer algorithm. *Period. Polytech. Electr. Eng. Comput. Sci.* **2022**, *66*, 1–17. [[CrossRef](#)]
42. Boudjema, Z.; Taleb, R.; Djerriri, Y.; Yahdou, A. A novel direct torque control using second order continuous sliding mode of a doubly fed induction generator for a wind energy conversion system. *Turk. J. Elec-Trical Eng. Comput. Sci.* **2017**, *25*, 965–975. [[CrossRef](#)]
43. El Ouanjli, N.; Aziz, D.; El Ghzizal, A.; Mohammed, T.; Youness, E.; Khalid, M.; Badre, B. Direct torque control of doubly fed induction motor using three-level NPC inverter. *Prot. Control Mod. Power Syst.* **2019**, *17*, 1–9. [[CrossRef](#)]
44. Benbouhenni, H.; Bizon, N. Advanced direct vector control method for optimizing the operation of a double-powered induction generator-based dual-rotor wind turbine system. *Mathematics* **2021**, *9*, 2297. [[CrossRef](#)]
45. Yaichi, I.; Semmah, A.; Wira, P.; Djerriri, Y. Super-twisting sliding mode control of a doubly-fed induction generator based on the SVM strategy. *Period. Polytech. Electr. Eng. Comput. Sci.* **2019**, *63*, 178–190. [[CrossRef](#)]
46. Benbouhenni, H. Synergetic control theory scheme for asynchronous generator based dual-rotor wind power. *J. Electr. Eng. Electron. Control. Comput. Sci.* **2021**, *7*, 19–28. Available online: <https://jeeccs.net/index.php/journal/article/view/215> (accessed on 9 April 2022).
47. Nnem, L.N.; Lonla, B.L.; Sonfack, G.B.; Mbih, J. Review of a Multipurpose Duty-Cycle Modulation Technology in Electrical and Electronics Engineering. *J. Electr. Eng. Electron. Control Comput. Sci.* **2018**, *4*, 9–18. Available online: <https://jeeccs.net/index.php/journal/article/view/101> (accessed on 9 April 2022).